Journal of Biomolecular NMR, 7 (1996) 335–340
ESCOM

J-Bio NMR 363

Secondary structure of β-hydroxydecanoyl thiol ester dehydrase, a 39-kDa protein, derived from H^{α}, C^{α}, C^{β} and CO signal assignments and the Chemical Shift Index: Comparison with the crystal structure*

Valérie Copié[a], John A. Battles[b], John M. Schwab[b] and Dennis A. Torchia[a,**]

[a]*Molecular Structural Biology Unit, National Institute of Dental Research, National Institutes of Health, Bethesda, MD 20892, U.S.A.*
[b]*Department of Medicinal Chemistry and Pharmacognosy, Purdue University, West Lafayette, IN 47907, U.S.A.*

Received 3 April 1996
Accepted 8 May 1996

Keywords: Triple-resonance spectroscopy; NMR signal assignment; Chemical Shift Index; Protein secondary structure

Summary

Nearly complete backbone ^{1}H, ^{15}N and ^{13}C signal assignments are reported for β-hydroxydecanoyl thiol ester dehydrase, a 39-kDa homodimer containing 342 amino acids. Although ^{15}N relaxation data show that the protein has a rotational correlation time of 18 ns, assignments were derived from triple-resonance experiments recorded at 500 MHz and pH 6.8, without deuteration. The Chemical Shift Index, CSI, identified two long helices and numerous β-strands in dehydrase. The CSI predictions are in close agreement with the secondary structure identified in the recently derived crystal structure, particularly when one takes account of the numerous bulges in the β-strands. The assignment of dehydrase and a large deuterated protein [Yamazaki et al. (1994) *J. Am. Chem. Soc.*, **116**, 11655–11666] suggest that assignment of 40–60 kDa proteins is feasible. Hence, further progress in understanding the chemical shift/structure relationship could open the way to determine the structures of such large proteins.

Escherichia coli β-hydroxydecanoyl thiol ester dehydrase is a 39-kDa homodimeric enzyme that plays a key role in anaerobic bacterial metabolism (Bloch, 1971). Dehydrase interconverts (*R*)-3-hydroxydecanoyl-ACP (ACP = acyl carrier protein, which is an intermediate in saturated fatty acid biosynthesis), with (*E*)-2-decenoyl-ACP and (*Z*)-3-decenoyl-ACP. (*E*)-2-Decenoyl-ACP is reduced to decanoyl-ACP, which is elaborated into the full-length saturated fatty acids. However, direct chain elongation of (*Z*)-3-decenoyl-ACP (i.e., without prior reduction of the double bond), leads to mono-unsaturated fatty acids, which are indispensable for the viability of the organism. This pathway is an alternative to the oxygen-dependent fatty acid desaturation process used by mammals. Since dehydrase is unique to bacteria, it is an attractive target for the design of new antibiotics.

When this project was initiated, there was virtually no information available about either the secondary or higher-order structure of dehydrase. Our initial goal was to determine the secondary structure of the protein by applying the Chemical Shift Index (Wishart et al., 1992; Wishart and Sykes, 1994) to the assigned backbone proton and carbon signals in order to identify α-helical and β-strand regions of the protein. By the time the project had been completed, an X-ray structure of dehydrase had become available (Leesong et al., 1996), enabling us to test the predictions of the CSI against the secondary structure seen in the crystalline state.

Another motivation for this work was to determine whether it would be possible to assign a 39-kDa protein without deuteration, using triple-resonance methods at a moderate field strength (500 MHz). These methods had previously been shown to be effective when applied to proteins having molecular weights up to 30 kDa (Grzesiek and Bax, 1992c; Fogh et al., 1994; Remerowski et al., 1994).

**Supplementary Material* is available on request, comprising Table S1 listing the spectral parameters; Table S2 listing the assignments; Fig. S1 showing the 2D ^{1}H-^{15}N HSQC spectrum; Fig. S2 showing sequential NOEs, secondary shifts, H-exchange and $^{3}J_{HN^{\alpha}}$ data; and Fig. S3 showing plots of the H^{α}, C^{α}, CO and C^{β} Chemical Shift Indexes.

**To whom correspondence should be addressed.

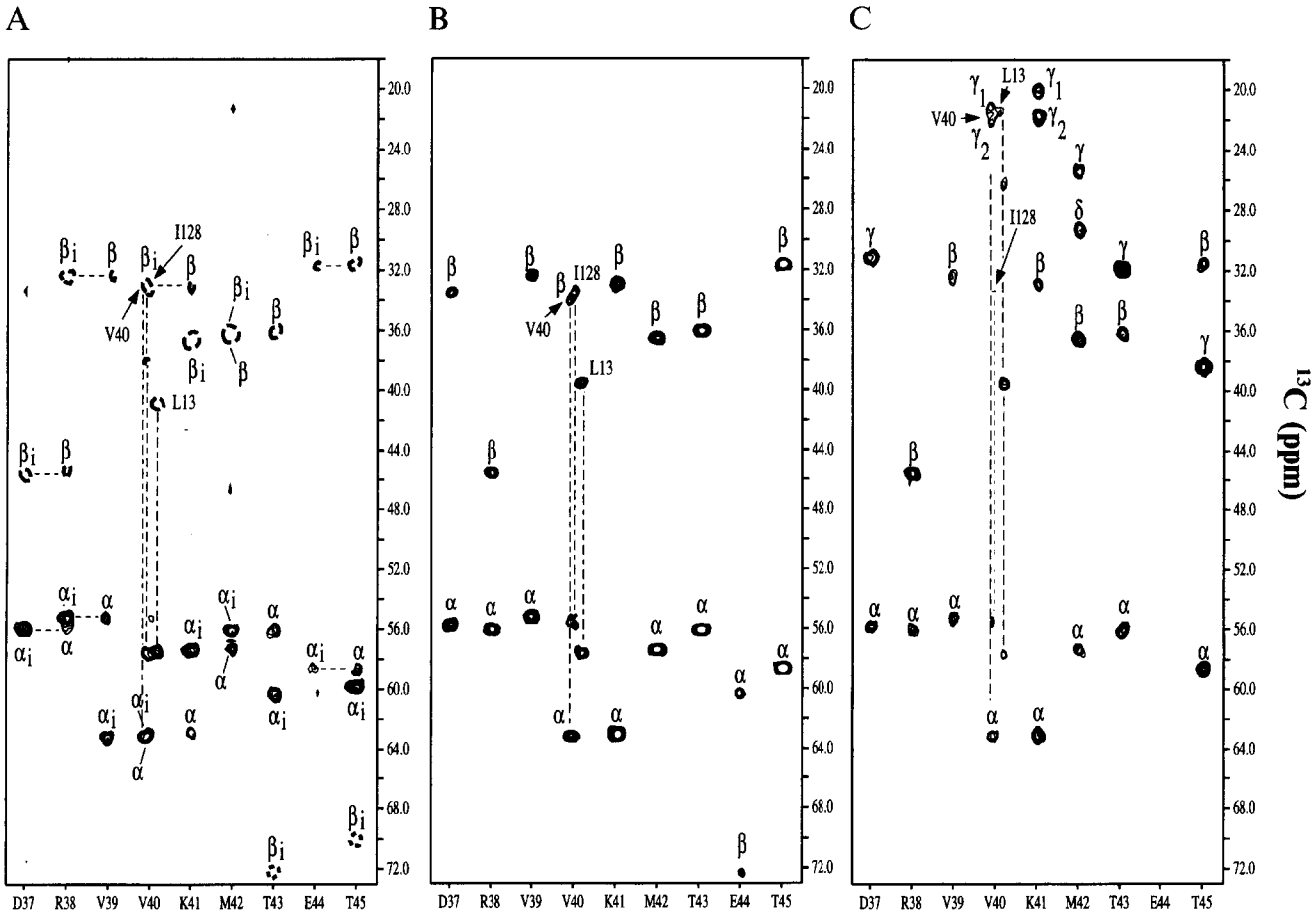

Fig. 1. Comparison of strips taken from (A) CBCANH; (B) CBCA(CO)NH; and (C) C(CO)NH spectra of dehydrase for residues Asp[37]–Thr[45]. Intraresidue connectivities are designated by the appropriate Greek letter with an i subscript, while sequential (i,i–1) connectivites are designated by the Greek letter alone. The beta-carbon correlations in panel (A) have negative signal intensities and are drawn as single dashed contours to indicate this fact. Spectral parameters are provided in Table S1.

Uniformly ^{15}N- and ^{15}N,^{13}C-labeled β-hydroxydecanoyl thiol ester dehydrase was produced by recombinant *E. coli* grown in M9 minimal medium, containing either $^{15}NH_4Cl$ (Cambridge Isotopes, Cambridge, MA) or $^{15}NH_4Cl$ and D-[$^{13}C_6$]glucose (Isotec Inc., Miamisburg, OH). The protein was purified as described previously (Cronan et al., 1988; Annand et al., 1993).

NMR spectra were recorded at 42 °C for aqueous solutions containing ca. 0.9 mM dehydrase (35 mg/ml) in either D_2O or H_2O/D_2O (95:5) containing 10 mM sodium phosphate, pH 6.8. Although a lower pH is more desirable to reduce the rate of amide proton exchange, it was found that protein solubility highly decreased at acidic pH values. The protein concentration was determined from the absorbance at 280 nm, using an extinction coefficient (Schwab et al., 1986) of 1.29 $l\,g^{-1}cm^{-1}$. All spectra were recorded on 220 µl solutions in 5 mm Shigemi NMR tubes. Assays showed no loss of enzyme activity after eight weeks of data collection at 42 °C.

All NMR spectra were recorded on Bruker AM and AMX-500 spectrometers, and were processed using nmrPipe (Delaglio et al., 1996) and PIPP (Garrett et al., 1991). The spectral parameters are listed in Table S1. Proton and ^{13}C chemical shifts, and CSI random-coil shifts (Wishart and Sykes, 1994) were referenced to TSP through water at 4.62 ppm (Ikura et al., 1990).

Each dehydrase monomer contains 171 amino acid residues (Cronan et al., 1988; Annand et al., 1993). Taking into account the N-terminal valine and the seven proline residues, 164 residues have potentially observable backbone NH correlations in a ^{1}H-^{15}N HSQC spectrum. We observed 155 backbone amide NH signals in the HSQC spectrum of dehydrase (Fig. S1). The excellent dispersion and sensitivity of the HSQC spectrum encouraged us to obtain sequential assignments of dehydrase, despite its size.

Sequential assignments of backbone amide proton and ^{15}N signals, as well as $^{13}C^{\alpha}$ and $^{13}C^{\beta}$ signals, were obtained from sequential connectivities observed in CBCANH (Grzesiek and Bax, 1992b) and CBCA(CO)NH (Grzesiek and Bax, 1992a) spectra. Taking into account the 24 glycine residues (no C^{β}), 7 proline residues (no NH), and N-terminal residues, these spectra can contain a maximum of 302 sequential and 300 intraresidue α/β correla-

tions, respectively. We observed 287 intraresidue $C^{\alpha i}/C^{\beta i}$ correlations and 240 interresidue $C^{\alpha i-1}/C^{\beta i-1}$ correlations in the CBCANH spectrum. In addition, 289 sequential C^{α}/C^{β} connectivities were observed in the CBCA(CO)NH spectrum. Starting points for sequential assignments were alanines, glycines, serines and threonines, because they have unique patterns of C^{α}/C^{β} chemical shifts. Using intraresidue $C^{\alpha i}/C^{\beta i}$ connectivities to identify one such type of residue, the α/β carbon chemical shifts of the preceding amino acid were identified from the $C^{\alpha i-1}/C^{\beta i-1}$ correlations observed in the CBCA(CO)NH spectrum. These chemical shifts were used to identify the intraresidue $NH/C^{\alpha}/C^{\beta}$ correlations of this residue in the CBCANH spectrum. Repeating this procedure linked the newly identified residue to the preceding residue, and in this manner stretches of sequentially linked amino acids were found. The types of amino acids in a stretch were identified using probabilities based upon C^{α}/C^{β} chemical shifts (Grzesiek and Bax, 1993a), and from side-chain carbon chemical shifts observed in a 3D C(CO)NH spectrum (Grzesiek et al., 1993). We illustrate the procedure, as well as the quality of the data, using strips for residues 37–45 of dehydrase taken from the CBCANH, CBCA(CO)NH and C(CO)NH spectra (Fig. 1).

Because of the high molecular weight of dehydrase, many correlations have modest or weak signal-to-noise ratios, particularly in the CBCANH spectrum. For example, only weak intraresidue α/β correlations are seen in the Glu^{44} strip, and sequential correlations are absent. However, clear sequential correlations link Glu^{44} to Thr^{43} in the CBCA(CO)NH spectrum and Thr^{45} to Glu^{44} in both the CBCA(CO)NH and C(CO)NH spectra (Figs. 1a and b). The problem of spectral overlap, as seen in the

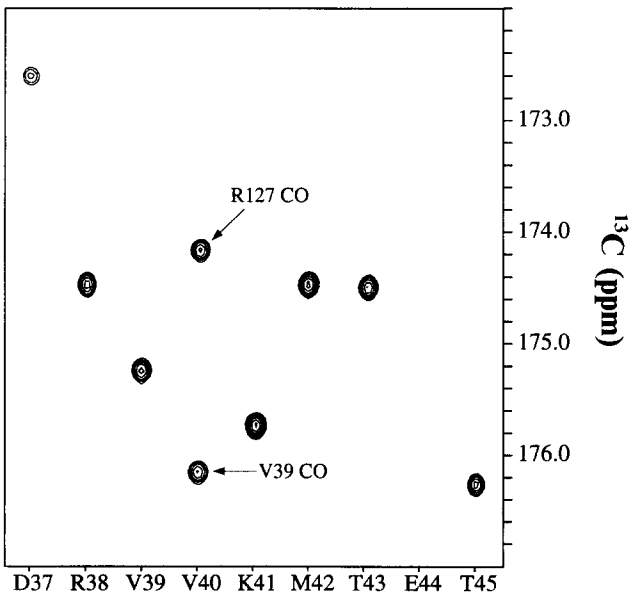

Fig. 2. Strips, taken from the 3D HNCO spectrum, used to obtain the CO signal assignments for residues Asp^{37}–Thr^{45}. Spectral parameters are provided in Table S1.

Val^{40} strip, which is nearly degenerate with that of Ile^{128}, was overcome by carefully examining the diagonal and cross-peak intensities in several adjacent ^{15}N planes.

Using the procedure outlined above, continuous stretches of amino acids were assigned from Asp^{2}–Gly^{25}, Gln^{27}–Leu^{28}, Ala^{30} (flanked by two prolines), Asn^{32}–Asn^{61}, Asp^{63}–Trp^{65}, Phe^{67}–Asp^{74}, Val^{76}–Met^{77}, Cys^{80}–Leu^{118}, Thr^{120}–Val^{134}, Leu^{138}–Phe^{165}, and Ser^{169}–Thr^{171}. Apart from amides in two isolated amino acids (Phe^{66} and Gly^{79}) and two segments, each three amino acids in length (Asn^{135}–Arg^{137} and Gln^{166}–Thr^{168}), all backbone amide proton and ^{15}N signals were assigned. The signals for these non-assigned amides were not observed, most probably because they exchange rapidly with water at pH 6.8. Signal assignments were checked by examining the carbon side-chain chemical shifts of the sequential correlations observed in the 3D C(CO)NH spectrum. As is clear in Fig. 1c, the carbon chemical shifts are fully consistent with the sequential assignments. In addition to enforcing the backbone assignments, the C(CO)NH spectrum also provided ^{13}C chemical shifts for most C^{γ} and C^{δ} signals.

The assignments of nearly every H^{α} and H^{β} and some H^{γ} signals were derived from 3D HBHA(CO)NH and ^{15}N HOHAHA-HSQC spectra, while the assignments were extended to backbone carbonyl carbons by recording 3D HNCO (Fig. 2) and HCACO spectra. Two 3D NOESY spectra were also recorded: a ^{15}N-separated NOESY-HSQC spectrum with water flip-back (Grzesiek and Bax, 1993b), and a 3D ^{15}N,^{13}C-separated NOESY/HSQC (Archer et al., 1993). The nearly two hundred d_{NN} and $d_{\alpha N}$ NOE connectivities derived from these spectra (Fig. S2) confirmed the assignments made by the heteronuclear J-correlation experiments and provided three additional α-proton assignments. The dehydrase signal assignments are listed in Table S2.

Using the nearly complete H^{α}, C^{α}, C^{β}, and CO signal assignments, the consensus CSI (Wishart and Sykes, 1994) was used to identify the secondary structure of dehydrase. The simplicity and tested reliability of this method (Wishart and Sykes, 1994) make it appealing, particularly in the case of a large homodimer where application of NOE-based structure methods is complicated by spin diffusion and the need to distinguish between intermonomer and intramonomer correlations. The α-helical and β-strand secondary structure elements identified by the consensus CSI (Wishart and Sykes, 1994) are listed in Table 1.

As seen in Table 1, the CSI predicts that dehydrase is a member of the α/β class of proteins, with two long α-helical segments and ten β-strands, six of which are each less than five residues in length. Examining the predictions of the individual CSI indices, one finds them to be in conflict about the presence of β-strands in several cases (Figs. 3 and S3). For example, the H^{α}, CO and C^{β} CSIs all predict that a β-strand extends from residues 37 through 42, whereas the CO CSI predicts that this entire

TABLE 1
COMPARISON OF RESIDUES IN HELIX/STRAND SECONDARY STRUCTURES IN DEHYDRASE*

Secondary structure	Residues		
	CSI[a]	X-ray[b]	Ideal(ϕ,ψ)[c]
Helix	9–15	9–16	9–16
		65–69	65–68
	80–98	79–96	79–96
		168–170	169
Strand	37–42	38–43	38,39,41–43
	51–58	53–59	52–59
	107–109	102–107	102,104,106–108
	111–114	110–113	110–113
	116–118		116–118
	124–129,132–134	123–135	123–129,132–134
	138–149	139–149	138–149
	155–158,161–164	152–165	155–158,161–165

The secondary structures were obtained by using either the backbone signal assignments and the consensus CSI or the crystal structure (Leesong et al., 1996).

[a] The consensus CSI program (Wishart and Sykes, 1994) was used to identify the secondary structure employing the Majority Rule. Residues were assigned as a helix only if at least two out of the three H^{α}, C^{α}, and CO CSIs indicated a helix. Residues were assigned as β-strand only if at least three out of the four H^{α}, C^{α}, C^{β}, and CO CSIs indicated a strand. Backbone assignments are complete except for the following ones: H^{α}, C^{α}, C^{β}, and CO of residues 78, 135, 136, 166, and 167; H^{α} of residue 77; and CO of residues 22, 61, 74, 77, and 165.

[b] Secondary structure as defined by PROCHECK (Kabsch and Sander, 1983; Laskowski et al., 1993).

[c] Residues which are either in helices or strands, according to either the CSI or PROCHECK, and have both their ϕ and ψ angles within ±45° of either those of an ideal α-helix (–57°,–47°) or those of an ideal antiparallel β-strand (–139°,135°).

region is a coil. In contrast, all four CSIs predict that residues 51–58 form a strand (Figs. 3 and S3). In order to better understand the patterns of the secondary chemical shifts, we examined the sequential connectivities observed in the 3D ^{15}N-separated and $^{15}N,^{13}C$ HSQC-NOESY spectra. Even limiting ourselves to a qualitative consideration of the NOE intensities, they provide insight into the cause of the variations in the predictions of the individual CSIs discussed above. For example, Fig. 4 shows strips taken from the ^{15}N-separated NOESY spectrum for residues 37 through 45. While strong $d_{\alpha N}$ connectivites are observed for residues (38,39), (39,40), (41,42) and (42,43), $d_{\alpha N}(37,38)$ and $d_{\alpha N}(40,41)$ connectivities are very weak. In addition, d_{NN} connectivities are observed for (37,38) and (40,41). By contrast, the NOESY spectrum of residues 52–59 shows an unbroken series of strong or medium $d_{\alpha N}$ connectivities and no d_{NN} connectivities (Fig. S2). Hence, the NOE data indicate that the 37–42 strand is distorted, probably by bulges, whereas the 51–58 strand is regular, in agreement with the secondary chemical shifts (Figs. 3 and S3) and with the CSI predictions. We note that the weak long-range $d_{NN}(38,57)$, $d_{NN}(41,55)$ and $d_{NN}(43,53)$ connectivities observed in both Fig. 4 and in the corresponding strips of residues 53–57 (spectrum not shown) suggest that strands 37–42 and 51–58 form a sheet. Finally, the NOESY spectrum also reveals weak $d_{\alpha N}(130,131)$, $d_{\alpha N}(131,132)$, and $d_{NN}(131,132)$ connectivities (Fig. S2); a result that is consistent with the break in the β-strand spanning residues 123–135, predicted by the CSI (Table 1).

The recent availability of the crystal structure of dehydrase (Leesong et al., 1996) permits the secondary structure identified by the CSI in solution to be compared with that seen in the crystal. The residues within the regular secondary structure in crystalline dehydrase, as assigned by using PROCHECK (Laskowski et al., 1993), are listed in the second column of Table 1. As can be seen when comparing columns 1 and 2 of Table 1, the two long α-helical domains observed in the crystal are identified by the CSI. While the CSI does not identify a short 3–10 helix spanning residues 65–69 in the crystal structure, this is apparently due to the fact that the small size of this domain severely restricts sampling by the CSI. In this particular case, 80% of the H^{α}, C^{α}, and CO CSI indices indicate that a helix spans residues 64–68; however, only the H^{α} CSI has the four consecutive helical indices required to define a helix. The requirement of four consecutive helical indices implies that the three-residue

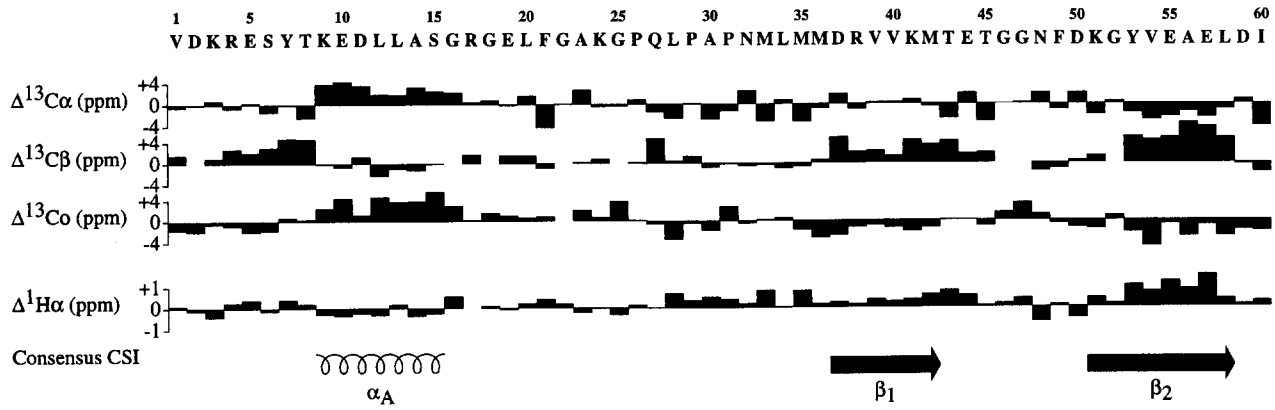

Fig. 3. Comparison of C^{α}, C^{β}, CO and H^{α} secondary chemical shifts observed for residues 1–60 of dehydrase. All measured secondary shifts, $^{3}J_{HNH^{\alpha}}$ coupling constants, slowly exchanging amide protons, and sequential NOE connectivities are provided in Table S2.

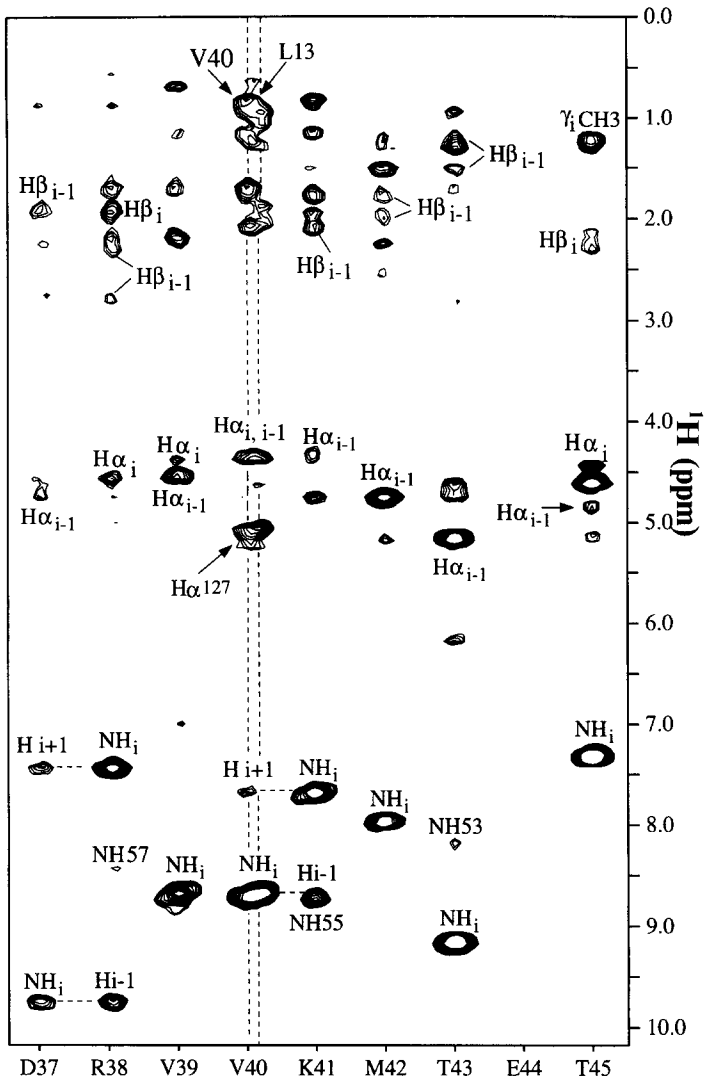

Fig. 4. Strips, taken from the 3D ^{15}N-separated NOESY/HSQC spectrum of dehydrase, for residues Asp^{37}–Thr^{45}. Spectral parameters are provided in Table S1.

C-terminal helix, found in the crystal structure, is too short to be recognized by the CSI. We note that the ^{15}N T_2 values of residues 170 and 171 are nearly 40% larger than the T_2 value of residues in the long helices, suggesting that these two residues are flexible in solution.

The discrepancy between the β-strands identified by the CSI and those observed in the crystal structure, as can be seen in Table 1, requires further discussion. Examination of the dehydrase crystal structure shows that this discrepancy is more apparent than real. The dehydrase structure has been described as a 'hot-dog' fold (Leesong et al., 1996), with a highly curved β-sheet (the roll) wrapping the long hydrophobic central helix (the hot dog). The sheet curvature is created by the presence of eight β-bulges (Leesong et al., 1996), and it is the distortions in the β-strands produced by the bulges that are the source of most of the differences between the β-strands identified by PROCHECK in the crystal structure and those identified by the CSI. It is interesting to note that if one lists only those residues in the strands that have (ϕ,ψ) values within ±45° of ideal β-sheet values (Table 1, column 3), they are in very good agreement with strand residues identified by the CSI. In fact, the breaks in the strands predicted by the CSI match several of the bulges observed in the crystal structure, e.g. at residues 130/131 and 159/160. In addition, it is seen that the short strand, 116–118, as identified by the CSI, but not by PROCHECK, does have (ϕ,ψ) values characteristic of a strand. It was not identified by PROCHECK, because residues 116–118 do not form β-sheet-type hydrogen bonds. Finally, we note that residues 135–137 and 166–168 are in exposed loops in the crystal structure, consistent with our hypothesis that rapid amide proton exchange is the reason that their NH NMR signals are not observed.

In conclusion, 3D heteronuclear triple-resonance experiments have provided nearly complete backbone and many side-chain signal assignments of the 39-kDa dehydrase homodimer in an efficient and reliable fashion.

We note that measurements of ^{15}N T_1 and T_2 values show that dehydrase does not have a particularly favorable correlation time for a protein of its size. The average T_1 (1.03 s) and T_2 (44 ms) values measured for sixteen well-resolved amides, located in either helices or strands, are simulated using the model-free approach (Lipari and Szabo, 1982) with $S^2 = 0.93$, $\tau_c = 18.7$ ns, $\tau_e = 0.1$ ns, r = 1.02 Å and ^{15}N CSA = 160 ppm. Alternatively, the average T_1/T_2 ratio of 23.5 ± 2.5 corresponds to an overall correlation time, τ_c, of 18.4 ± 1 ns at 42 °C. By comparison, $\tau_c = 14.5$ ns for the 37-kDa trpR complex (Yamazaki et al., 1994) at 37 °C. The larger-than-expected value of τ_c for dehydrase is ascribed to the shape of the molecule. The moments of inertia calculated from the X-ray coordinates (Leesong et al., 1996) show that dehydrase has the shape of an axially symmetric ellipsoid, with a ratio of semi-minor to semi-major axes of 0.62. For such an ellipsoid, the effective value of τ_c, obtained from average T_1 and T_2 values, calculated taking into account the orientation of each NH bond relative to the long axis of the ellipsoid (Woessner, 1962), is almost 20% larger than the τ_c value of a sphere of equal volume.

The CSI, in conjunction with the backbone assignments, identified the two major α-helical domains of the protein, as well as the extensive, but irregular β-strand structure of the protein. Small differences in solution and crystal structure or flexibility (e.g. at the C-terminus) may contribute to differences in the secondary structures identified by the CSI and PROCHECK. Not surprisingly, the internal consistency of the CSI indicators was highest (over 90% agreement) in regions of the sequence composed of lengthy and highly regular secondary structures (the two long helices and strands 51–58 and 138–149). Continued progress in relating chemical shifts to protein structure (Oldfield, 1995; Wishart et al., 1995) may allow for identification of bulges, various types of turns or loops, and tertiary structure. Combining this information with long-range NOE constraints, obtained from spectra of protonated and deuterated (Grzesiek et al., 1995; Venters et al., 1995) proteins, has the potential to provide solution structures of homodimeric, and possibly monomeric, proteins of larger than 40 kDa.*

Acknowledgements

We thank Geerten Vuister and Stephan Grzesiek for pulse sequences, Frank Delaglio and Dan Garrett for NMR processing software and Rolf Tschudin for expert technical support. We thank Janet L. Smith and Minsun Leesong for kindly providing the coordinates of the dehydrase crystal structure, prior to publication. This work was supported by the Intramural AIDS-Targeted Anti-Viral Program of the Office of the Director of the National Institutes of Health, and by NIH Grant GM 36286 (to J.M.S.).

Note added in proof

After submitting this manuscript, the assignments and secondary structure of 4-oxalocrotonate tautomerase, a 41-kDa homohexamer containing $6 \times 62 = 372$ amino acid residues, were reported (Stivers et al., 1996).

References

Annand, R.R., Dozlowski, J.F., Davisson, V.J. and Schwab, J.M. (1993) *J. Am. Chem. Soc.*, **115**, 1088–1094.

Archer, S.J., Vinson, V.K., Pollard, T.D. and Torchia, D.A. (1993) *Biochemistry*, **32**, 6680–6687.

Bloch, K. (1971) *The Enzymes*, **5**, 441–464.

Cronan, J.E., Li, W.B., Coleman, R., Narasimhan, M., de Mendoza, D. and Schwab, J.M. (1988) *J. Biol. Chem.*, **263**, 4641–4646.

Delaglio, F., Grzesiek, S., Vuister, G., Zhu, W., Pfeifer, J. and Bax, A. (1996) *J. Biomol. NMR*, **6**, 277–293.

Fogh, R.H., Schipper, D., Boelens, R. and Kaptein, R. (1994) *J. Biomol. NMR*, **4**, 123–128.

Garrett, D.S., Powers, R., Gronenborn, A.M. and Clore, G.M. (1991) *J. Magn. Reson.*, **95**, 214–220.

Grzesiek, S., Anglister, J. and Bax, A. (1993) *J. Magn. Reson.*, **101**, 114–119.

Grzesiek, S. and Bax, A. (1992a) *J. Am. Chem. Soc.*, **114**, 6291–6293.

Grzesiek, S. and Bax, A. (1992b) *J. Magn. Reson.*, **99**, 201–207.

Grzesiek, S. and Bax, A. (1992c) *J. Magn. Reson.*, **96**, 432–440.

Grzesiek, S. and Bax, A. (1993a) *J. Biomol. NMR*, **3**, 185–204.

Grzesiek, S. and Bax, A. (1993b) *J. Am. Chem. Soc.*, **115**, 12593–12594.

Grzesiek, S., Wingfield, P., Stahl, S., Kaufman, J.D. and Bax, A. (1995) *J. Am. Chem. Soc.*, **117**, 9594–9595.

Ikura, M., Kay, L.E. and Bax, A. (1990) *Biochemistry*, **29**, 4659–4667.

Kabsch, W. and Sander, C. (1983) *Biopolymers*, **22**, 2577–2637.

Laskowski, R.A., MacArthur, M.W., Moss, D.S. and Thornton, J.M. (1993) *J. Appl. Crystallogr.*, **26**, 283–291.

Leesong, M., Henderson, B.S., Gillig, J.R., Schwab, J.M. and Smith, J.L. (1996) *Structure*, **4**, 253–264.

Lipari, G. and Szabo, A. (1982) *J. Am. Chem. Soc.*, **104**, 4546–4559.

Oldfield, E. (1995) *J. Biomol. NMR*, **5**, 217–225.

Remerowski, M.L., Domke, T., Groenewegen, A., Pepermans, H.A.M., Hilbers, C.W. and Van de Ven, F.J.M. (1994) *J. Biomol. NMR*, **4**, 257–278.

Schwab, J.M., Ho, C.-K., Li, W.-B., Townsend, C.A. and Salituro, G.M. (1986) *J. Am. Chem. Soc.*, **108**, 5309–5316.

Stivers, J.T., Abeygunawardana, C., Whitman, C.P. and Mildvan, A.S. (1996) *Protein Sci.*, **5**, 729–741.

Venters, R.A., Metzler, W.J., Spicer, L.D., Mueller, L. and Farmer II, B.T. (1995) *J. Am. Chem. Soc.*, **117**, 9592–9593.

Wishart, D.S., Richards, F.M. and Sykes, B.D. (1992) *Biochemistry*, **31**, 1647–1651.

Wishart, D.S. and Sykes, B.D. (1994) *J. Biomol. NMR*, **4**, 171–180.

Wishart, D.S., Bigam, C.G., Holm, A., Hodges, R.S. and Sykes, B.D. (1995) *J. Biomol. NMR*, **5**, 67–81.

Woessner, D.E. (1962) *J. Chem. Phys.*, **37**, 647–654.

Yamazaki, T., Lee, W., Arrowsmith, C.H., Muhandiram, D.R. and Kay, L.E. (1994) *J. Am. Chem. Soc.*, **116**, 11655–11666.